

Concept and development of multifunctional hybrid systems: Photoswitchable and thermotunable plasmonic materials

M Nguyen, L Boubekeur-Lecaque, C Mangeney, A Chevillot-Biraud, F Maurel, N Félidj, J Aubard

▶ **To cite this version:**

M Nguyen, L Boubekeur-Lecaque, C Mangeney, A Chevillot-Biraud, F Maurel, et al.. Concept and development of multifunctional hybrid systems: Photoswitchable and thermotunable plasmonic materials. Plasmonics in Chemistry and Biology, edité par M. Lamy de la Chapelle et N. Félidj, Edition PAN Stanford, 2019., In press, 9780429458750. hal-03705877

HAL Id: hal-03705877
https://hal.science/hal-03705877

Submitted on 27 Jun 2022

HAL is a multi-disciplinary open access archive for the deposit and dissemination of scientific research documents, whether they are published or not. The documents may come from teaching and research institutions in France or abroad, or from public or private research centers.

L'archive ouverte pluridisciplinaire **HAL**, est destinée au dépôt et à la diffusion de documents scientifiques de niveau recherche, publiés ou non, émanant des établissements d'enseignement et de recherche français ou étrangers, des laboratoires publics ou privés.

Concept and development of multi-functional hybrid systems: Photoswitchable and thermotunable plasmonic materials

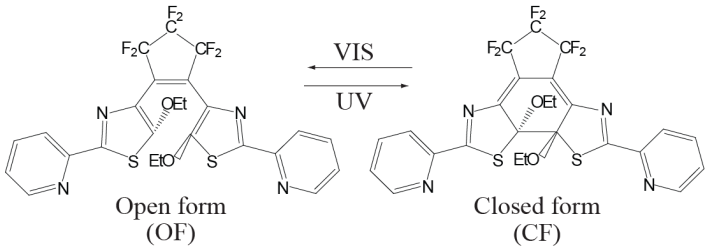
*M. Nguyen,[1,2] L. Boubekeur-Lecaque, [1] C. Mangeney, [1] A. Chevillot-Biraud, [1] F. Maurel, [1] N. Félidj[1] and J. Aubard[1]**
[1]*Laboratoire ITODYS, Université Paris Diderot, Sorbonne Paris Cité, CNRS UMR 7086, 15 rue Jean–Antoine de Baïf, 75205 Paris Cedex 13, France*
[2] *Present address: University of Science and Technology of Hanoi, Vietnam Academy of Science and Technolgy, 18 Hoang Quoc Viet, Cau Giay, Ha Noi, Viet Nam*
(*) jean.aubard@univ-paris-diderot.fr

1.1 INTRODUCTION

In a previous chapter of this book [1] it was demonstrated how to process thermoresponsive plasmonic nanostructures by grafting PNIPAM on GNPs arrays†. Various applications were proposed to show the interest of this approach for developing new plasmonic systems for (bio) molecular sensing and enhanced spectroscopies (mainly SERS). To go further in designing multifunctional hybrid systems based on gold NPs arrays covered by PNIPAM, recent works have suggested to attach organic molecules with specific properties at the end of this polymer chains. Thus, plasmonic systems based on GNPs substrates covered by thermoresponsive polymer brushes labeled with photochromic units could lead, using suitable LSPR excitation, to new enhanced molecular (optical) properties [2]. Last but not least these hybrid systems are of great interest because they could exhibit both photoswitchable and thermotunable LSPR optical changes. The choice of light sensitive molecules attached to plasmonic nanostructures comes from the great interest in the design, functioning and applications of optical switches

† See all the abbreviations at the end of the text

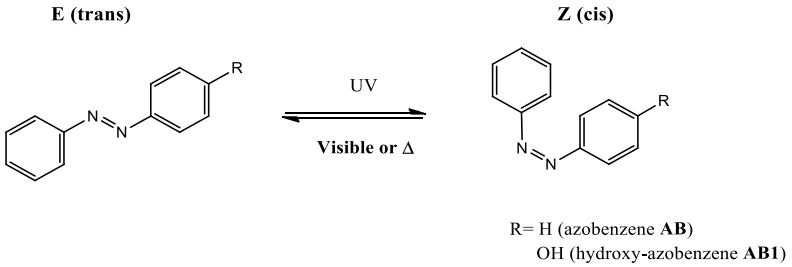
and electronic devices at the nanoscale [3]. In this context, organic photochromes are good candidates since specific changes in their electronic and structural properties occur under light irradiation [4].
Photochromism of organic compounds is defined as a reversible transformation induced in one or both direction by light between two isomeric states with different properties, such as change in their geometry, polarity, UV-Vis absorption bands etc… Among various series of organic photochromes, diarylethenes (scheme 1) have received increasing attention during the past twenty years thanks to their interesting optical and photochromic properties, which make them promising candidates for optical switches and memories [5].



Scheme 1. Reversible photoisomerization in diarylethenes family upon UV-Vis light irradiation.

Unfortunately, due to the lack of suitable commercially available diarylethene derivatives that can be used for the attachment process (through an efficient click chemistry approach), azobenzenes (AB) molecules have been preferred for practical reasons: Azobenzenes form one of the largest and most studied classes of photochromic molecules [6]; they have been used as, light triggered switches in a variety of polymers, surface-modified materials, protein probes, molecular machines, holographic recording devices and metal ion chelators. AB exhibits remarkable photostability as negligible decomposition occurs even after prolonged irradiation. Moreover, large amount of various azobenzene derivatives are commercially available, particularly the hydroxy derivative which leads in a one step synthesis to the alkyne derivative, which can be easily used in a click chemistry synthesis (*vide infra,* scheme 4). AB molecules exist in two isomeric states, *trans* and *cis*, with the former being ~10 kcal/mol more stable than the latter. The *trans*

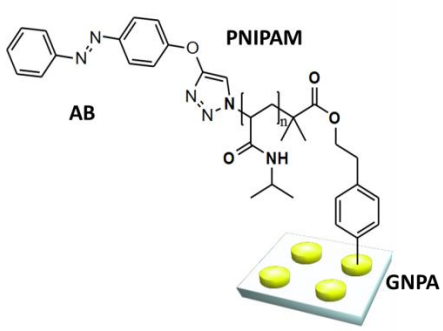
to *cis* photoisomerization of azobenzenes is induced by UV irradiation (*e.g.* 365 nm) while visible light (>460 nm) reversibly transforms *cis* to *trans* (scheme 2). These isomers have a different spatial arrangement of the aromatic moieties (scheme 2) and show significantly different physical and chemical properties; thus, the *trans* to *cis* isomerization is accompanied by a considerable change in polarity, from zero dipole moment of the *trans* isomer to ~3 D for the dipole moment of the *cis* form. However, the optical changes on going from *trans* to *cis* isomer are weak (*i.e.* UV-Vis absorption band, Raman spectra, IR absorption…) and its photochromic efficiency is quite low. Moreover, depending on the nature of the substituents on the aromatic groups, azobenzenes can undergo thermal *cis* to *trans* isomerization at room temperature [6].



Scheme 2. Reversible isomerization of azobenzene moieties upon UV-Vis irradiation. The *trans (E)* isomer is planar and the *cis* (Z) isomer is bent and more compact.

In this chapter we report on the procedure to attach onto lithographically designed gold NPs arrays a thermoresponsive polymer, poly(N-isopropylacrylamide), PNIPAM, functionalized with an azobenzene (AB) chromophore at the end of the polymer chains (scheme 3). The optical properties of the gold NPs (namely LSPR) and SERS spectra of attached AB molecules were investigated after photoirradiation (UV and visible) in air at room temperature and in water upon heating. It was observed that efficient *cis* to *trans* photoisomerisation takes place due to LSPR excitation and probably originated from a coupling mechanism between GNPs and azobenzenes. Moreover, since the distance between the photoactive AB moiety and the gold NPs decreases upon heating above the critical temperature (LCST)

of PNIPAM, it is expected that the coupling efficiency between them should increase as well. [7,8] Indeed, it was shown in previous papers, dedicated to optical properties of PNIPAM-GNPs plasmonic systems [1,7-8], that the distance between the plasmonic GNPs arrays and the polymer end groups can be modulated upon increasing/decreasing the temperature around the LCST of PNIPAM. Thus, taking into account that the distance between the GNPs and the photochromic unit plays a major role in the coupling strength, such a thermal modulation of the distance should lead to observable modifications of optical properties of the hybrid system, *i.e.* LSPR spectral changes and photochromic efficiency.



Scheme 3. Illustration of the attachment of an azobenzene derivative on PNIPAM brushes grafted on GNP Arrays.

In the following we will detail the fabrication and implementation of a three component system coupling GNPs of 2D lithographic arrays to photochromic units through a PNIPAM linker. Optical properties of this multifunctional hybrid system were obtained thank to UV-visible absorption and surface enhanced Raman scattering (SERS) spectroscopies.

1.2 ELABORATION AND PROPERTIES OF THE MULTIFUNCTIONAL HYBRID SYSTEM

The Photochrome–PNIPAM-Au hybrid system was built through a bottom-up approach involving (see scheme 3, above), i) the fabrication of

plasmonic substrates consisting of gold nanoparticle arrays (GNPAs), ii) the chemical surface modifications of GNPs for the covalent bonding of a thermo-responsive organic linker (PNIPAM) and iii) the selective covalent attachment of azobenzene (AB) photochromes at the end of the polymer chains).

1.2.1 *Preparation of gold nanoparticle arrays (GNPAs)*

The electron beam lithography (EBL) method to prepare GNPs arrays was detailed previously [1]. Extinction spectra of four GNPAs along with the AFM image of one selected array (D140) are shown in Fig 1.

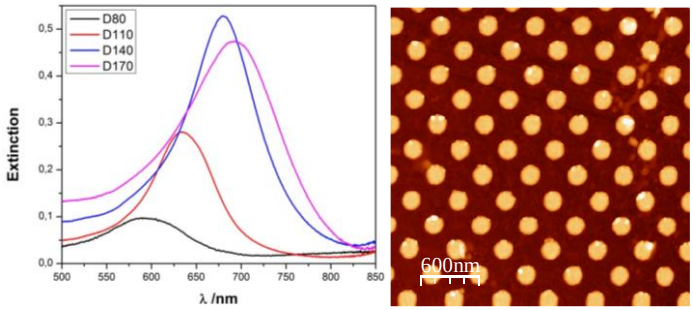
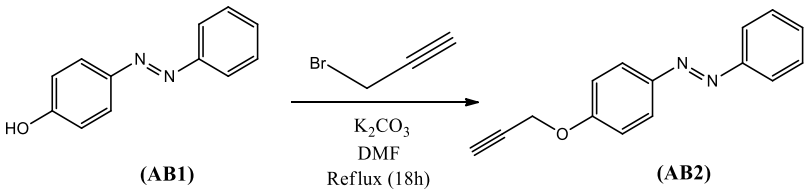


Figure 1. (a) Extinction spectra of four GNPAs (disk diameter D= 80, 110, 140 and 170 nm) recorded in air at room temperature. These spectra were recorded with a spectrometer (LOT ORIEL, 74050 model, 400-1000 nm spectral range) equipped with a CCD camera (ANDOR, CCD-8855) under an upright optical microscope (Olympus, BX51TF) through a 100 x objective (Olympus, NA: 0.8) (b) AFM image of one array (D140) obtained in air at room temperature.

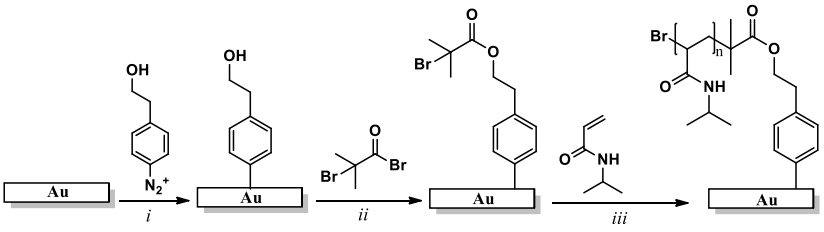
1.2.2 *Preparation of GNPs arrays covered by PNIPAM with AB chromophore end group (GNPA-PNIPAM-AB)*

The stepwise strategy for the preparation of the multifunctional hybrid plasmonic system consists in two major steps: (1) the grafting of PNIPAM chains on the GNPA, (2) the attachment of the alkyne azobenzene derivative (AB2, obtained from 4-phenylphenol, AB1, scheme 4) at the end of the polymer chain.



Scheme 4: From 4-phenylphenol (AB1) a one-step synthesis (nucleophilic substitution by propargyl bromide) leads to the alkyne azobenzene derivative (AB2).

This multistep functionalization is summarized in Fig 2. It involves, (i) a spontaneous covalent grafting of hydroxyl (–OH) terminated aryl diazonium moieties on the surface of the GNPs; (ii) the terminal hydroxyl groups are treated with 2-bromoisobutyryl bromide leading to bromo-terminated ester groups able to initiate the polymerization of NIPAM. Using this approach, the grafting of polymerization initiators could be confined exclusively on the gold nanoparticle surface. (iii) PNIPAM brushes are grown from the initiators using standard aqueous Surface-Initiated Atom Transfer Radical Polymerization (SI–ATRP) conditions. In the step (iv), substitution of the bromo-end groups (of PNIPAM brushes) by azide provided the "click-active" substrates. Then, the azide-terminated substrates were reacted with azobenzene AB2 in typical click-chemistry conditions (azide-alkyne cycloaddition, step v) to yield azobenzene-terminated gold NPs array abbreviated as **GNPA-PNIPAM-AB**.



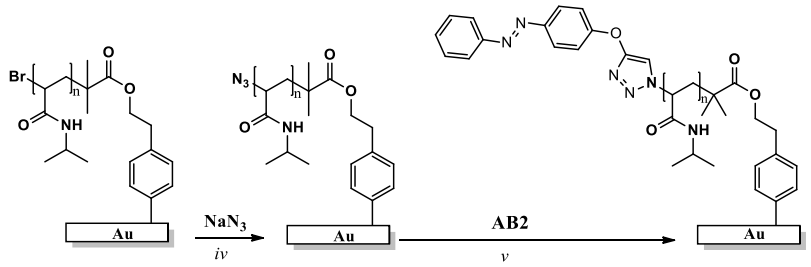


Figure 2. General scheme summarizing the stepwise strategy for the preparation of the multifunctional hybrid plasmonic system (**GNPA-PNIPAM-AB**). (i) spontaneous covalent grafting of hydroxyl (–OH) terminated aryl diazonium on the surface of the GNPs; (ii) 2-bromoisobutyryl bromide (0.1 M, toluene), trimethylamine (0.12 M), 5 min. (iii) NIPAM in Surface-Initiated Atom *Trans*fer Radical Polymerization (SI–ATRP) conditions. (iv) NaN_3 (0.05 M, DMF) for 24 h, rt (v) β-cyclodextrin (1.25 mM), AB2 (0.05 M), Cu(II) sulfate pentahydrate (2.5 mM), L-ascorbic acid sodium salt (7.5 mM) in water under Ar at room temperature, 24 h.

1.2.3 *AFM and optical (extinction) characterization of the thermosensitive properties of the GNPA-PNIPAM-AB system*

The thickness of PNIPAM grafted on GNPA was measured by AFM in air at room temperature. The AFM images of GNPA recorded before and after grafting of PNIPAM allow estimating the dry PNIPAM thickness which is around 5 nm (in air at room temperature, PNIPAM adopts a collapsed conformation [9]). It should be noted that the height of the dried organic coating estimated to ca. 15±2 nm (Fig 3) reflects the total thickness including the initiator layer and the polymer brushes. This value, which represents the distance between the AB chromophore and the GNP surface (see, scheme 3), is very close to the near field area (*ca.* 10 nm) and it is expected that a quite strong coupling strength should take place between AB and gold NPs.

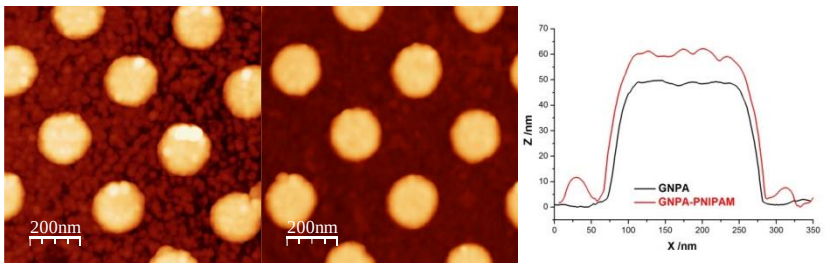


Figure 3. AFM images and height profiles in air at room temperature of GNPA (left and black curve) and GNPA-PNIPAM (right and red curve).

In order to characterize the thermosensitive properties of the system, we considered its optical extinction changes with temperature in water. At room temperature in water (below the LCST) the PNIPAM adopts a swollen (extended) conformation. From the AFM measurements in air at room temperature (in dry condition the polymer is collapsed, see Fig 3) and taking into account that the swelling ratio, α, defined as $\alpha=h_{swollen}/h_{dry}$ (where $h_{swollen}$ and h_{dry} corresponds to the swollen and dry brush thickness), was estimated to *ca.* 2 [9], the PNIPAM thickness in water at room temperature was estimated to *ca.* 10 ± 2 nm. Thus, in these conditions, the total length of the spacer can be estimated to 20 ± 2 nm (at room temperature in water). Increasing the external temperature up to 50°C in water (above the LCST of PNIPAM) induces a dramatic change in the polymer state which adopts a collapsed conformation of which the thickness significantly decreases upon heating to, 5 ± 2 nm.

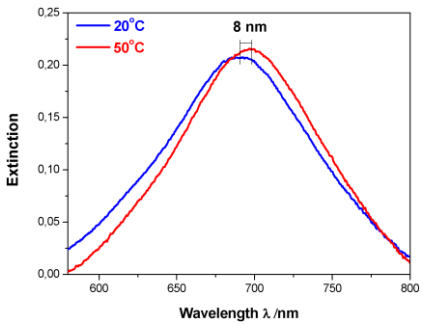


Figure 4. Changes with temperature of the extinction spectra of a ***GNPA-PNIPAM-AB*** sample (array D140) in water at 20 °C (blue line) and 50°C (red line). Extinction spectra of GNPAs in water at various temperature were recorded using a 100 x immersion objective (Olympus, N.A: 1).

Thus for ***GNPA-PNIPAM-AB*** samples, under controlled conditions in water, the spacer length was reduced from 20 nm (at room temperature) to 15 nm after heating above the LCST (at 50°C). The extinction spectra, for one selected array (D140), recorded in water at 20 and 50°C, are shown in Fig 4. From these spectra it appears that LSPR bands are quite sensitive to the conformation change of PNIPAM around LCST since, depending on the arrays, LSPR is red-shifted by 8-10 nm upon heating. Moreover, cycling experiments (not shown) evidenced that LSPR thermal switching of the ***GNPA-PNIPAM-AB*** system is reversible and reproducible [9]. This bathochromic shift with temperature is due to a change of the medium index in the vicinity of GNPs by conformational change of the polymer. The medium index becomes larger by heating above the LCST, due to the collapse of PNIPAM.

1.3 REVERSIBLE CHANGES OF THE LSP RESONANCE OF GNPA-PNIPAM-AB UPON *CIS*/*TRANS* ISOMERIZATION OF AZOBENZENE

In order to carry out the isomerization of azobenzene (AB) units the samples were photo-irradiated in air at room temperature and in water upon heating. Light irradiations (UV or visible) were performed using a spot light source (Hamamatsu, Lightningcure, LC8, equipped with a 200 W Xe-Hg lamp) through a NIR long pass filter, to protect samples from thermal effects, and appropriate band pass filters to select either UV (365 nm) or visible (540 nm) light, before reaching the sample.

Fig 5a shows extinction spectra recorded in air, of one selected ***GNPA-PNIPAM-AB*** sample (array D140) after UV (365 nm) and visible (540 nm) light irradiations for 90 min. For all samples, a small but reproducible blue shift of the LSPR band, depending on the arrays, is observed when going from *trans* to *cis* isomer upon 365 nm irradiation. Green light irradiation induced a reversible switching with a

bathochromic shift of the LSPR band, which returns to the initial *trans* position value (see cycling experiments in the inset of Fig 5a). These blue/red reproducible shifts, recorded upon cycling UV/Vis light irradiations, which are related to changes in the refractive index of AB in the environment of GNPs could be assigned for the blue shift to a less conjugated bent structure of the *cis* isomer while the *trans* isomer which is endowed with a highly conjugated planar structure (see scheme 2) leads, as expected, to a bathochromic (red) shift.

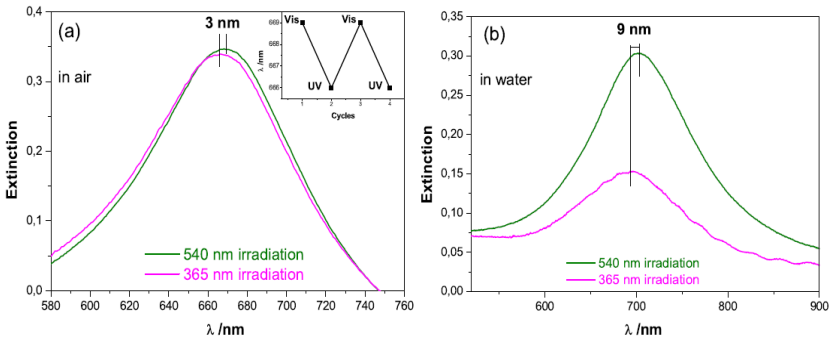


Figure 5. (a) Extinction spectra of a ***GNPA-PNIPAM-AB*** sample (array D140) upon repetitive cycling irradiations to UV (365nm, pink line) and visible (540nm, green line) each of 90 min duration. (a) Recorded in air at room temperature (20°C); the reproducible cycles are shown in the inset. (b) Recorded in water at room temperature (20°C); poor reproducibility of the cycles in this case (not shown). Either in air or in water, exposure to UV light led to *cis* isomer with a blue shift of the LSPR band while 540 nm green light led to *trans* isomer with a red shift of similar amount.

Extinction spectra, for all sample arrays were recorded in water at room temperature after 365/540 nm cycling irradiation (Fig 5b). For all samples blue/red shifts are measured in the range, *ca.* 5-20 nm, but with a poor reproducibility. Surprisingly, these shifts are slightly more important than those measured in air at the same temperature where the dry polymer is shrunk (collapsed). On going from air to water the LSPR band makes a large move towards the red for more than 20-40 nm, depending on the arrays, and as well known the LSPR sensitivity to the medium increases in the red/IR part of the spectrum. Thus, although the spacer length increases in water at 20°C (20 nm *vs.* 15 nm in air), the

spectral shifts induced upon UV/Vis light irradiation are (slightly) greater than those measured in air.

Upon heating up to 50°C in water the distance between the photoactive AB moiety and the GNP is reduced from 20 to 15 nm (*vide supra*) a value very close to the near field area and it is expected that the concomitant increase in the coupling strength should lead to more important changes of LSPR band of ***GNPA-PNIPAM-AB***, upon 365/540 nm light irradiations, than those observed at room temperature. Surprisingly, extinction spectra recorded at 50°C in water showed no significant (convincing) difference with the LSPR changes at 20°C in water upon 365/540 nm cycling irradiations for all samples. The reason for this failure is unclear but could be due to the damage of the samples after long UV irradiations along with hundred UV/Vis cycles.

Anyway, is it so surprising to not observe larger changes in the LSPR band on going from 20°C to 50°C in water after 365/540 nm light irradiations for all samples ?: It is known that EM field enhancement increases as the distance to the GNP core decreases and in the present case it is more or less expected an increase in the E field intensity, felt by the AB unit at the end of the PNIPAM chain, of about $(70/65)^3$, *i.e.* 1.25 (see further on in the text, eq. 1.1). Thus, the related expected "stronger" coupling strength should be difficult to observe with the low LSPR sensitivity of the ***GNPA-PNIPAM-AB*** system, upon 365/540 nm light irradiations.

Therefore, to follow reversible *trans/cis* photoisomerization of AB in our hybrid system we turn towards SERS detection which is expected to probe the reversible photoswitching of a very small amount of AB attached to the PNIPAM linker.

1.4 SERS EXPERIMENTS OF GNPA-PNIPAM-AB AT VARIOUS TEMPERATURES AND UPON AB *CIS*/*TRANS* ISOMERIZATION

1.4.1 *Thermo-induced reversible changes of azobenzene SERS intensity*

SERS experiments with ***GNPA-PNIPAM-AB*** samples were carried out in air at room temperature and in water upon heating below and above the LCST of PNIPAM. Azobenzene molecules used in this study, *i.e.* AB1, AB2 and the AB unit in ***GNPA-PNIPAM-AB*** samples, display

fluorescence properties and it was "difficult" in these conditions to record Raman spectra using 633 nm laser excitation. On the contrary, NIR excitation at 785 nm provides satisfactory Raman spectra (see for example the Raman spectrum of AB2 powder in Fig 6b). Unfortunately, for ***GNPA-PNIPAM-AB*** samples, excitation at 785 nm led to SERS spectra showing huge and wide Raman bands in the 1300-1600 cm^{-1} spectral range arising from amorphous carbon layers which develop at the sample surface due to thermal degradation, thus preventing good quality SERS spectra to be recorded. Therefore, all SERS experiments with ***GNPA-PNIPAM-AB*** samples were conducted with 633 nm laser excitation. In these conditions, SERS spectra appear with a strong background attributed to surface enhanced fluorescence (SEF) which is spectrally modified by LSPR excitation [10]; however, as discussed further on in the text, 633 nm excitation is able to induce some *cis* to *trans* photoisomerization, depending both on the laser power and on the acquisition time. Fig 6a shows SERS spectra in water at temperatures below and above the LCST of PNIPAM (resp. 20 and 54 °C) for one selected sample (array D140). All SERS spectra display the characteristic Raman lines of similar azobenzene derivatives [11] and, as evidenced in Fig 6b, there is a one to one correspondence with the six strong lines of the Raman spectrum of AB2 powder at *ca.*, 1142 and 1186 cm^{-1} (CN stretching modes), 1414 and 1441 cm^{-1} (ring modes coupled to N=N stretching), 1464 cm^{-1} (N=N stretching) and 1595 cm^{-1} (ring modes, C=C stretching).

Despite the small amount of AB units (estimated to less than 5 in a 10 nm^2 area, [9]), located at the end of each polymer chain, SERS spectra recorded in the 700- 1700 cm^{-1} range are of enough good quality to allow some quantitative analysis. Thus, it appears clearly that the SERS intensities increase with temperature on going from 20°C (below the LCST) to 54°C (above the LCST of PNIPAM). Cooling down the substrate to room temperature leads to a decrease of the SERS signal reversibly to the initial intensity recorded below the LCST. A two-fold increase of the Raman band intensities is then detected, which is in perfect agreement with the theoretical enhancement, *ca.* 2.4, calculated from a simple EM model, which is now detailed just below.

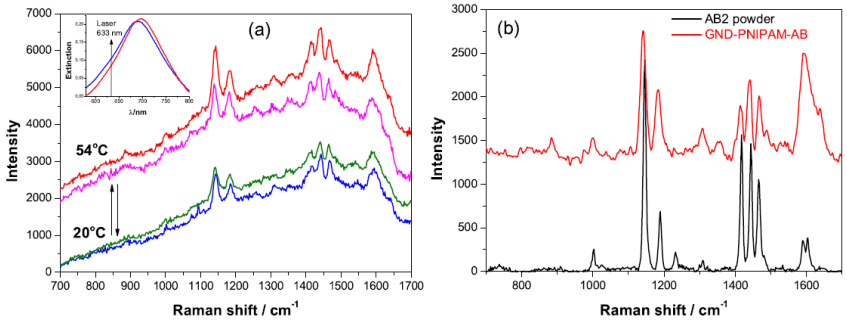


Figure 6. (a) SERS spectra excited at 633 nm, for one selected ***GNPA-PNIPAM-AB*** sample (array D140) in water after several 54/20°C heating /cooling cycles. The LSPR bands (in water at 20 and 54°C) are shown in the inset. (b) Raman spectrum of AB2 powder (785 nm excitation, black curve) and the SERS spectrum of a ***GNPA-PNIPAM-AB*** sample in water at 54°C (red curve). The SERS Spectrum, excited at 633 nm, is corrected from the strong fluorescence

In this model, the GNPAs were modelized as a collection of regular hemi-spheres, schematically represented in Fig 7. In these conditions one can defined, $A(\nu)$, the local E-field enhancement factor at a frequency ν and at a distance r from the NP center, as [12]:

$$A(\nu) = (\varepsilon - \varepsilon_0 / \varepsilon + 2\varepsilon_0)\,(a/r)^3 \qquad (1.1)$$

where ε represents the dielectric function of the metal, ε_0 the dielectric function of the surrounding medium and a the radius of the hemi-spheric NPs.

The corresponding SERS enhancement, G^{EM}, can thus be approximated as [12]:

$$G_{SERS}^{EM} \approx |A(\nu_0)|^4 = \left| \frac{\varepsilon(\nu_0) - \varepsilon_0}{\varepsilon(\nu_0) + 2\varepsilon_0} \right|^4 \left(\frac{a}{r}\right)^{12} \qquad (1.2)$$

where $A(\nu_0)$, is the local E-field enhancement factor at the incident laser frequency, ν_0 . This formula, known as the E^4 rule for SERS enhancement factor [12], shows that the Raman gain falls rapidly with the distance r between the probe molecule and the GNP center. If we now consider the two situations experienced by the ***GNPA-PNIPAM-AB*** samples in

water, *i.e.*, (1) when the PNIPAM brushes are collapsed at 50 °C with r_1= 65 nm and (2) when the PNIPAM brushes are swollen at 20 °C with r_2= 70 nm, the expected increase for SERS intensities can be expressed as: $\mathbf{I_1/I_2 = (r_2/ r_1)^{12} = 2.4}$; where $\mathbf{I_1}$ and $\mathbf{I_2}$ are the SERS intensity at 50 °C and 20°C, respectively. It should be noted that this simple EM SERS calculation predicts that on increasing the temperature from 20 to 50 °C it is expected a two fold increase in SERS intensity, in agreement with the experimental results from Fig 6a. Moreover, these results clearly indicate that AB units are effectively located at PNIPAM end groups.

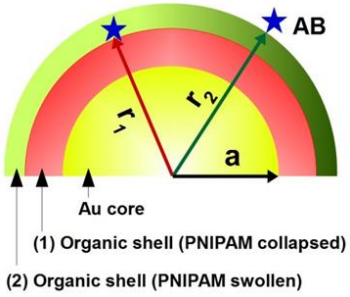


Figure 7. Schematic representation of a hemi-sphere GNP surrounded by an organic shell with a AB photochromic unit. Where a is the radius of the hemi-spheric NP; $\mathbf{r_1}$ and $\mathbf{r_2}$ the distance from the AB unit to the GNP center, in the collapsed (1) and swollen (2) state of PNIPAM.

Since the organic coating layer thickness was reduced from 20 nm (at room temperature) to 15 nm after heating above the LCST, SERS intensities easily probe this distance modulation induced by the thermo responsive polymer. The full reversibility of the system was demonstrated by several heating/cooling cycles, as shown below in figure 8 and this definitely confirms that AB molecules are tightly attached at the end of PNIPAM chains.

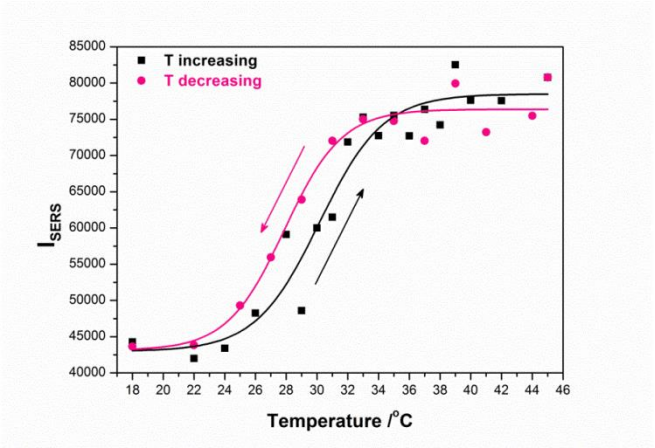


Figure 8. Integrated SERS intensity, of the 1142 cm^{-1} Raman line of AB, versus temperature for one selected ***GNPA-PNIPAM-AB*** sample (D 140).

1.4.2 *SERS intensity changes upon cis/trans isomerization of azobenzene*

Several 365/540 nm light irradiation cycles were then performed on various ***GNPA-PNIPAM-AB*** samples and probed by SERS. First, these experiments were carried out in air at room temperature to verify that SERS intensity changes were able to monitor the reversible *cis/trans* photoisomerization of azobenzene units [11]. Those experiments were performed in water at 20°C and at 54°C, below and above the LCST of PNIPAM respectively, to detect how the SERS spectra could be changed or modulated by both 365/540 nm photoirradiation and heating.

Fig 9 shows SERS spectra of a selected sample after UV (365nm) and green (540nm) light irradiations in air at room temperature. At room temperature in air PNIPAM adopts a collapsed conformation with a polymer thickness of 5±2 nm (*vide supra*). Because, i) the total distance between the AB chromophore and the GNPA is *ca.*15±2 nm (see Fig 4, AFM height profiles) and is very close to the near field area (*ca.* 10 nm) and ii) the 633nm excitation was within the LSPR band of this sample (*ca.* 670 nm in air, Fig 5a), these conditions should allow for high SERS enhancement for the ***GNPA-PNIPAM-AB*** sample under study. When this sample was UV irradiated for an hour the SERS spectrum (*cis* form) immediately collected showed a higher intensity, by nearly 2-fold (Fig 9,

left), than the SERS spectrum obtained before UV irradiation (*trans* form). The reasons why the SERS intensity of the *cis* isomer is higher than the *trans* is not clear but enhanced charge *trans*fer of the *cis* state (high dipole moment) along with its bent conformation becoming closer to the GNP core could be at the origin of the higher SERS intensity of the *cis* form. Moreover, these SERS intensity changes recorded upon cycling UV/Vis light irradiations can be likely related to the blue/red shift of the LSPR band. Upon 365 nm irradiation the formation of *cis* isomer led to a blue shift of the LSPR band and thus to a better matching with the 633 nm excitation, leading to a SERS intensity increase. Green light irradiation induced a reversible switching with a bathochromic (red) shift of the LSPR band, which returns to the initial *trans* position value with the concomitant decrease, as observed, of the SERS intensity. These observations show that the analysis of SERS intensities could be able to probe the reversible *cis/trans* photoswitching of a very small amount of AB attached to the end of PNIPAM polymer chains.

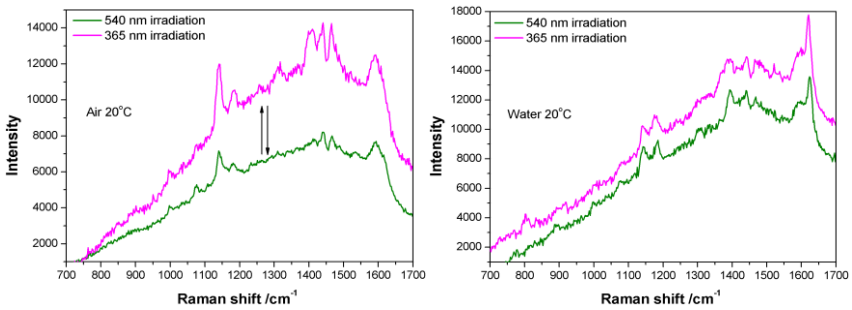


Figure 9. SERS spectra excited at 633 nm, of a selected ***GNPA-PNIPAM-AB*** sample (array D140), upon repetitive cycling irradiations to UV (365nm, pink line) and visible (540nm, green line) light, each of 1h duration. Spectra were recorded in air (left) and in water (right), at room temperature (20°C).

Similar SERS experiments were carried out upon 365/540 nm irradiation in water at 20 and 54°C. SERS spectra of the same selected sample (array D140), recorded after UV (365nm) and green (540nm) light irradiation in water at room temperature are shown in Fig 9 (right). It should be noted that these SERS spectra, recorded at 20°C in water upon 365/540 nm cycling irradiations, are almost identical and showed no significant SERS intensity difference.

On going from air to water the LSPR band makes a large move towards the red for more than 30-40 nm, depending on the arrays (see Fig 5b). In these conditions there is a total mismatch between LSPR (*ca.* 700-710 nm) and laser excitation (633 nm) and a weak EM and molecular coupling takes place, thus leading to poor SERS spectra with no significant difference in intensity between *trans* or *cis* isomer. Moreover, in water at room temperature (below the LCST) the PNIPAM adopts a swollen (extended) conformation with a thickness estimated to *ca.* 10 ± 2 nm and, in these conditions, the total length of the organic linker can be estimated to 20±2 nm, further contributing to the decrease of the SERS intensities with respect to those obtained in air at room temperature. Increasing the temperature up to 50°C in water induces a conformation change of PNIPAM (collapsed state) and the distance between the photoactive AB moiety and the GNP unit is reduced to *ca.* 15nm (*vide supra*) and it is expected that the concomitant increase in the coupling strength should lead to more important changes in the SERS intensities, upon 365/540 nm light irradiation, than those observed at room temperature. Unfortunately, no significant difference with the SERS spectra at 20°C in water was observed upon reversible cycling photoirradiations at 50°C for all ***GNPA-PNIPAM-AB*** samples.

In these SERS studies of covalently attached AB moieties in ***GNPA-PNIPAM-AB*** samples after photoirradiation (UV and visible) in air at room temperature and in water upon heating, promising results were obtained and deserve to be summarized here:

(i) Reproducible SERS intensities, of the AB chromophore, easily probe the distance modulation induced by the thermo responsive polymer after several reversible 54/20°C heating /cooling cycles in water.

(ii) The analysis of SERS intensity changes of ***GNPA-PNIPAM-AB*** upon 365/540 nm irradiation in air at room temperature could be a way to follow the reversible *cis/trans* photoswitching of a very small amount of AB attached to the end of PNIPAM polymer chains. Further experiments are necessary to check the reproducibility of those results.

(iii) As with LSPR detection we failed to observe any SERS spectral modification at 50°C upon 365/540 nm irradiation in water. Even with the SERS detection, the ***GNPA-PNIPAM-AB*** system is not enough sensitive to detect the influence of thermal switching on AB photoisomerization in water.

1.5 CONCLUSION AND FUTURE DEVELOPMENTS

All the experiments reported here, are in correct agreement with previous recent results either on related photochromic-PNIPAM-Au [13] or in similar Au-SAM-AB systems [11,14] even if these latter studies highlight some contradictory results with ours. However, as reported by others, SAMs linker as well as PNIPAM in the present work both ensure reversible *trans/cis* photoswitching of AB upon UV/Vis light irradiation. Interestingly, since the polymer thickness varies with temperature around the LCST, a plasmonic system including PNIPAM is dual and able to respond to both photoirradiation and thermal stimuli. Moreover, although this point is never pointed out in the abundant literature, investigation of AB photoswitching in SAMs is hampered by the fact that exposure to UV light in air causes irreversible damage to the SAMs by oxidation of the thiol bond. This point could perhaps explain some discrepancies and contradiction as compared to previously reported results concerning AB photoswitching. [11,14]. Furthermore our study highlights an important point in the context of applications to the development of nano-photoswitching or molecular electronic devices: the PNIPAM based plasmonic hybrid system, ***GNPA-PNIPAM-AB*** does not suffer from extensive UV degradation and the covalent grafting of this linker onto the GNP substrate ensures longer time stability than the common thiol-based SAMs linker. Finally, the reason for some reverse trends in our results is unclear and need further studies with more suitable EBL arrays and other photochromic systems such as diarylethenes which show very efficient photoisomerization process and large optical contrast between isomers [15,16]. Therefore, to follow reversible *trans/cis* photoisomerization of AB in our hybrid system we turned towards SERS detection which was expected to probe the reversible photoswitching of a very small amount of AB attached to the PNIPAM linker with enhanced sensitivity. Unfortunately, even with SERS detection we were unable to detect the influence of thermal switching on AB photoisomerization in the ***GNPA-PNIPAM-AB*** system in water.

Some important points remain and need to be overcome to improve this thermo and photo-sensitive hydrid plasmonic system. In particular, for the development of applications (*e.g.*, optical switches and electronic devices at the nano scale) one needs to detect the photochromic state non

destructively and this implies to use NIR-SERS excitation. Indeed, as already mentioned above in the main text, SERS excitation at 633 nm is able to induce some *cis* to *trans* photoisomerization, depending on the laser power and on the acquisition time. Unfortunately, it was very difficult to obtain good quality SERS spectra of ***GNPA-PNIPAM-AB*** at 785 nm because of the rapid thermal degradation of polymer layers preventing to make any quantitative analysis. Therefore, all SERS experiments with ***GNPA-PNIPAM-AB*** samples were conducted at 633 nm laser excitation with short acquisition time (1- 4s) and low laser power (*ca.* 65 µW at the sample), thus allowing SERS spectra to be recorded with moderate fluorescence (SEF) background and probably very limited *cis* to *trans* photoisomerization. Unfortunately, in these recording conditions, 633nm SERS spectra are of medium (low) quality and reliable SERS intensity analysis are "difficult" and it is hopeless in those conditions to detect the weak specific Raman features of *cis* isomer [11].

Finally, improvement of the thermo and photo-sensitive hydrid plasmonic system using NIR-SERS detection needs further studies with more suitable EBL arrays and different photochromic systems, such as diarylethenes which show very efficient photoisomerization process and large SERS contrast between isomers [17]. Furthermore, a higher PNIPAM thickness difference, between the collapsed and swollen state, might also be taken into account: rather than the actual 5/10 nm it would be better to try with 10/20 nm [13]; in this latter case the theoretical EM SERS calculation (*vide supra*) predicts that on increasing the temperature from 20 to 50 °C a fivefold increase in SERS intensity could be observed. Such experiments are currently underway.

Abbreviations

AB: Azobenzene
AFM: Atomic force microscopy
ATRP: Atomic *Trans*fer Radical Polymerization
CE: Chemical enhancement
DS: Diazonium salt
EBL: Electron-beam Lithography
EE: Electromagnetic enhancement
EF: Enhancement factor
GNPs: Gold nanoparticles
GNPAs: Gold nanoparticle arrays
LCST: Lower critical solution temperature
LSP: Localized Surface Plasmon
LSPR: Localized Surface Plasmon Resonance
NPs: Nanoparticles
PNIPAM: poly-N-Isopropylacrylamide
SAMs: self assembled molecules
SI-ATRP: Surface-initiated atomic *trans*fer radical-polymerization
SEF: Surface-enhanced fluorescence
SERS: Surface-enhanced Raman scattering
XPS: X-ray photoelectron spectroscopy

1.6 REFERENCES

1. Nguyen, M. *et al.*, Thermosensitive polymer-coated plasmonic nanostructures for reversible confinement biomolecules, *this book*.
2. Ueno, K and Misawa, H. *(2013).* Surface plasmon-enhanced photochemical reactions, *J. Photochem. Photobiol., **C***, pp. 15, 31– 52.
3. Feringa, B. L. (2001) *Molecular Switches* (Wiley-VCH Verlag GmbH, Darmstadt).
4. Crano, J. C. and Guglielmetti, R. J. (1999) *Organic Photochromic and Thermochromic Compounds*, volume 1 and 2 (Plenum Press, New York).
5. Irie, M. (2000). Diarylethenes for Memories and Switches, *Chem. Rev.*, **100**, pp. 1685–1716.
6. Bandara, H. M .D. and Burdette, S. C. (2012) Photoisomerization in different classes of azobenzene, *Chem. Soc. Rev.*, **41**, pp. 1809–1825.
7. Gehan, H, Fillaud, L. Chehimi, M. Aubard, J. Hohenau, A. Felidj, N. and Mangeney, C. (2010). Thermo-induced Electromagnetic Coupling in Gold/Polymer Hybrid Plasmonic Structures Probed by Surface-Enhanced Raman Scattering, *ACS Nano,* **4**, pp. 6491–6500.
8. Gehan, H. Mangeney, C., Aubard, J.,Lévi, G., Hohena, A., Krenn, J. R., Lacaze, E. and Félidj, N. (2011) Design and Optical Properties of Active Polymer-Coated Plasmonic Nanostructures, *J. Phys. Chem. Lett.*, **2**, pp. 926–931
9. Nguyen, M., Kanaev, A., Sun, X., Lacaze, E., Lau-Truong, S.,Lamouri, A., Aubard, J., Felidj, N., Mangeney, C. (2015) Tunable Electromagnetic Coupling in Plasmonic Nanostructures Mediated by Thermoresponsive Polymer Brushes, *Langmuir*, **31**, pp. 12830−12837
10. Le Ru, E. C., Etchegoin, P. G., Grand, J., Félidj, N., Lévi, G. (2007) Mechanisms of Spectral Profile Modification in Surface-Enhanced Fluorescence, *J. Phys. Chem. C*, **111**, pp. 16077-16079.
11. Joshi, G. K., Blodgett, K. N., Muhoberac, B. B., Johnson, M. A., Smith, K. A., Sardar, R. (2014) Ultrasensitive photoreversible molecular sensors of azobenzene-functionalized plasmonic nanoantennas, *Nano Lett.*, **14**, pp. 532–540.
12. Le Ru, E. C., Grand, J., Félidj, N., Aubard, J., Lévi, G., Hohenau, A., Krenn, J.R., Blackie, E. and Etchegoin, P. G. (2009) Experimental verification of the SERS electromagnetic model beyond the $|E|^4$ approximation: Polarisation effect, *J. Phys. Chem.C*, **112**, pp. 8117-8121.
13. Imao, S., Nishi, H. and Kobatake, S. (2013) Thermo-and photoresponsive reversible changes in localized surface plasmon resonance of gold nanoparticles covered by poly(N-isopropylacrylamide) with photochromic diarylethene end group, *J. Photochem. Photobiol.,* A, 252, pp. 37–45.
14. Zheng, Y. B., Payton, J. L., Chung, C.H., Liu, R. Cheunkar, S., Pathem, B. K., Yang, Y., Jensen, L. and Weiss, P. S. (2011) Surface-Enhanced Raman Spectroscopy to Probe Reversibly Photoswitchable Azobenzene in Controlled Nanoscale Environments, *Nano Lett.*, **11**, pp. 3447–3452.
15. Boubekri, R., Yasukuni, R., Lau Truong, S., Grand, J., Perrier, A., Maurel, F. and Aubard, J. Raman (2013) Study of a photochromic diarylethene

molecule: a combined theoretical and experimental study, *J. Raman Spectrosc.*, **44**, pp. 1777–1785

16. Yasukuni, R., Boubekri, R., Grand, J., Felidj, N., Maurel, F., Perrier, A., Métivier, R., Nakatani, K., Pei, Yu. and Aubard, J. *(2012)* Specific and Nondestructive Detection of Different Diarylethene Isomers by NIR-SERS, *J. Phys. Chem. C*, **116**, pp. 16063–16069.
17. Yasukuni, R., Ouhenia-Ouadahi, K., Boubekeur-Lecaque, L., Félidj, N., Maurel, F., Métivier, R., Nakatani, K., Grand, J. and Aubard, J. (2013) Silica-Coated Gold Nanorod Arrays for Nanoplasmonics Devices, *Langmuir*, **29**, pp.12633−12637.